Steady state mode-locking of the $Nd:YVO_4$ laser operating on the 1.34 µm transition using intracavity SHG in BIBO or PPMgSLT

Hristo Iliev,[a)] Ivan Buchvarov,[a)] Veselin Alexandrov,[a)] Sunao Kurimura,[b)] Valentin Petrov[c)]

[a]Department of Quantum Electronics, Faculty of Physics, Sofia University,
5 James Bourchier Blvd., BG-1164 Sofia, Bulgaria;
[b]Advanced Materials Laboratory, National Institute for Materials Science,
1-1 Namiki, Tsukuba 305-0044, Japan;
[c]Max-Born-Institute for Nonlinear Optics and Ultrafast Spectroscopy,
2A Max-Born-Str., D-12489 Berlin, Germany

ABSTRACT

Passive mode-locking of Nd-lasers operating on the $^4F_{3/2} \rightarrow {}^4I_{13/2}$ transition is problematic for semiconductor saturable absorber mirrors (SESAMs) not only because of difficulties in their fabrication process but also in relation to the achievable parameters and damage resistivity. We investigate an alternative approach based on second-order nonlinearity inside the laser cavity which utilizes negative $\chi^{(2)}$-lens formation in a SHG crystal assisted by nonlinear reflection of the so-called "frequency-doubling nonlinear-mirror" (FDNLM). This approach has been previously employed only for mode-locking of Nd-lasers emitting at 1.06 µm. Here we demonstrate passive mode-locking of a diode-pumped $Nd:YVO_4$ laser operating at 1342 nm based on negative $\chi^{(2)}$-lensing assisted by the FDNLM effect. Using a 7-mm-long BiB_3O_6 (BIBO) nonlinear crystal or 10-mm-long and 1-mm-thick periodically-poled Mg-doped stoichiometric lithium tantalate (PPMgSLT) crystal and output couplers highly-reflecting at the second-harmonic with optimized transmission at the fundamental, we achieve average output powers in the steady-state mode-locked regime of the order of 1 W at pulse durations in the 4-7 ps range. Such a combination of high output power and short pulse duration is superior with respect to the results previously reported with SESAM mode-locked Nd-lasers operating on this transition. Higher average powers have been obtained for this laser transition only by the complex additive mode-locking technique. In our case the average power limit is set by the maximum power achievable in the fundamental transversal mode in the continuous-wave (CW) regime. The shortest pulses (FWHM of 3.7 ps) can be very well fitted by $sech^2$ temporal shape assumption.

Key words: mode-locked lasers; Nd-lasers; diode-pumping.

1. INTRODUCTION

In the last decade, there is growing interest in steady-state mode-locking of diode-pumped Nd-lasers operating on the $^4F_{3/2} \rightarrow {}^4I_{13/2}$ transition around 1.3 µm. Such laser sources could be useful for a number of applications in semiconductor industry, telecommunications and medicine. Active mode-locking using amplitude or frequency modulation was the first technique applied to such diode-pumped lasers[1] but it provides in general relatively long pulses if compared to the bandwidth supported by the emission spectrum.

The first passive mode-locking technique applied to diode-pumped 1.3 µm Nd-lasers in the steady state regime was additive mode-locking[2] and although this technique is scalable in power,[3] it is a complex and not very practical approach employing single-mode fibers in a coupled cavity and locking electronics. The much simpler for realization semiconductor saturable absorber mirror (SESAM) mode-locking is widely used near 1 µm but the spectral region around 1.3 µm is problematic because of difficulties in the fabrication process and damage resistivity. With increasing

Solid State Lasers XX: Technology and Devices, edited by W. Andrew Clarkson, Norman Hodgson, Ramesh Shori,
Proc. of SPIE Vol. 7912, 79120T · © 2011 SPIE · CCC code: 0277-786X/11/$18 · doi: 10.1117/12.879179

Downloaded from SPIE Digital Library on 25 Feb 2011 to 62.44.99.208. Terms of Use: http://spiedl.org/terms

the operating wavelength, technical and engineering problems occur, generally limiting the optical quality of the SESAMs. In fact, each SESAM is designed and fabricated to operate only at a specific wavelength and it is difficult to optimize its modulation depth independently of the nonsaturable losses. The first demonstration of continuous-wave (CW) SESAM mode-locking of a Nd-laser operating near 1.3 µm was in 1996.[4] In this work, stable mode-locked operation of Nd:YVO_4 and Nd:YLF lasers was reported, with relatively low output powers of 50 and 130 mW, respectively. Pulse durations as short as 4.6 ps in the case of Nd:YVO_4 and 5.7 ps in the case of Nd:YLF were achieved. Subsequently, few other reports on mode-locked operation of 1.3 µm Nd-lasers by different types of SESAMs appeared, basically trying to improve their performance in terms of average output power and long term stability.[5-7] The highest average output powers (1.05 W at 152 MHz) were demonstrated only recently,[8] with an AlGaInAs based SESAM, however, the pulse duration from this Nd:YVO_4 laser amounted to 26.4 ps.

In this work we investigate an alternative passive mode-locking technique based on second-order nonlinearity inside the laser cavity which utilizes $\chi^{(2)}$-lens formation in a second-harmonic generation (SHG) crystal[9] assisted by the nonlinear reflection of the so-called Frequency Doubling Nonlinear Mirror (FDNLM). This approach is generally free of spectral limitations and absorption problems, and enables easier power scaling to the multi-watt level. The same technique has been previously used for mode-locking of Nd-lasers emitting at 1.06 µm.[10,11] It should be emphasized that this hybrid approach is distinctly different from the FDNLM mechanism acting alone because the SHG takes place far from perfect phase-matching. Indeed, mode-locking of a 1.3 µm Nd-laser by the FDNLM alone has been achieved only in the non-stationary regime with pulsed (lamp-) pumping.[12] Here we demonstrate stable CW mode-locking of a diode-pumped Nd:YVO_4 laser operating at 1.342 µm with an average output power of ~1 W and pulse durations as short as ~4 ps, which, if compared to Ref. 4 and 8, means that for the first time high average powers and short pulse durations are simultaneously available from a passively mode-locked 1.3-µm Nd-laser source.

2. EXPERIMENTAL SET-UP

The laser cavity is schematically shown in Fig. 1. The active element (AE) is a 9 mm long, *a*-cut, 1.5°-wedged Nd:YVO_4 crystal with 0.25 at. % doping. The end faces were antireflection (AR) coated for minimum losses at the laser wavelength. The laser crystal was mounted in a Cu holder whose temperature was stabilized at 20°C by circulating water. The Nd:YVO_4 laser was longitudinally pumped by the unpolarized radiation of a 808 nm laser diode bar coupled into a 400 µm optical fiber (NA=0.22). The output beam from the optical fiber was focused by a 1:1 reimaging unit and delivered onto the Nd:YVO_4 crystal through the plane end mirror M which transmits the pump radiation (Fig. 1).

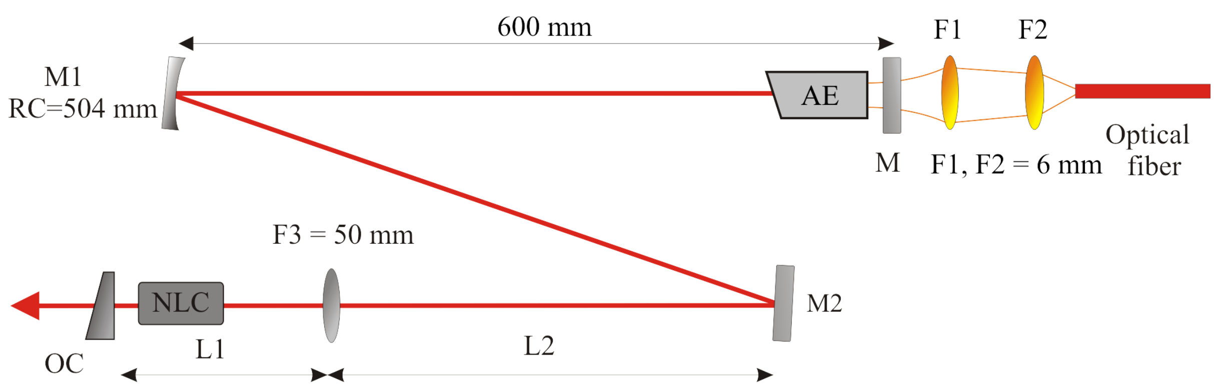

Fig. 1. Schematic of the laser cavity: F1, F2 - pump objective, AE - Nd:YVO_4 active element, M, M1, M2 - highly reflecting mirrors, F3 - focusing lens, NLC – nonlinear crystal, OC - output coupler. The physical cavity length amounts to 1.23 m. L1=71 mm, L2=320 mm (NLC ≡ BIBO) and L1=75 mm, L2=315 mm (NLC ≡ PPMgSLT).

As nonlinear crystal (NLC) we employed a 7-mm long bismuth triborate BiB_3O_6 (BIBO) with an aperture of 3×3 mm^2 cut at θ=9° and φ=0° in the *x-z* plane for type-I oo-e phase-matching and a 10-mm long periodically-poled 1 mol. %

Downloaded from SPIE Digital Library on 25 Feb 2011 to 62.44.99.208. Terms of Use: http://spiedl.org/terms

MgO-doped stoichiometric lithium tantalate $LiTaO_3$ (PPMgSLT) with a thickness of 1 mm along the z-axis and a width of 5 mm. Both crystals were AR-coated for the fundamental and the second harmonic wavelengths. In the case of BIBO, phase-matching was adjusted by the critical angle θ, while the temperature was held at 25°C through precise control (±0.5°C) of the temperature of the water circulating through the Cu-holder. In the case of PPMgSLT, whose period (14.7 μm) was designed for phase-matched SHG at 1342 nm at a temperature of 188°C, phase-matching was controlled by the temperature of the crystal holder.

The radius of curvature (RC) of the folding mirror M2 (RC=504 mm), the focal length of the AR-coated intracavity lens F3, and the separations given in Fig. 1 were chosen to ensure beam radii of ~80 μm in the nonlinear crystal and ~200 μm in the position of the active element AE. Plane mirrors with different characteristics were employed as output couplers (OC). The Nd:YVO_4 laser operates in π-polarization.

3. EXPERIMENTAL RESULTS AND DISCUSSION

In the case of PPMgSLT, the measured second-harmonic (SH) power versus temperature (Fig. 2) shows maximum conversion efficiency at T_{max}=461.5±1 K (holder temperature) and a FWHM of ΔT_{FWHM}=4.6 K for the phase-matching curve. Stable passive mode-locking operation was observed, however, at higher temperatures, at T_{ML}=467.5±1 K, depending on the OC used. This corresponds to SHG far from perfect phase-matching, in the first maximum of the temperature-dependent phase-matching curve. The phase-mismatched SHG introduces $\chi^{(2)}$-nonlinear lens effect in the laser resonator.[9] Operation on the right wing of the phase-matching curve corresponds to a negative $\chi^{(2}$-lens formation.

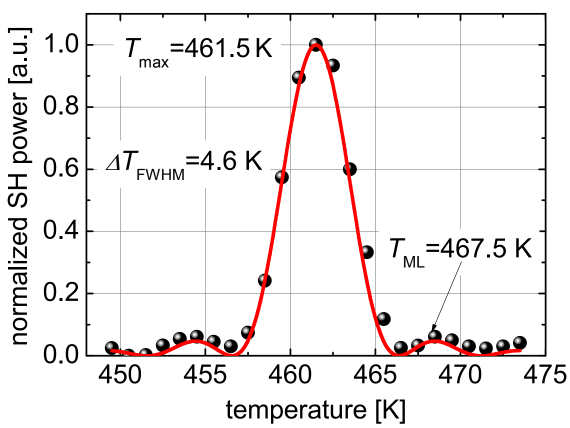

Fig. 2. Normalized single-pass second-harmonic (SH) intensity as a function of the PPMgSLT crystal holder temperature measured in the CW regime with a 5% OC that has a leakage of about 1% at the SH. The red curve is a theoretical fit.

The existing temperature dependent Sellmeier equations of SLT[13] predict a phase-mismatch of 4.18±0.6 rad at T_{ML}=467.5 K corresponding to mode-locking. A very similar value of ~3.9 rad is obtained with θ=0.64 rad/K for the phase-mismatch coefficient, derived by fitting the experimental data in Fig. 2 with the theoretically calculated single-pass SHG signal as a function of $\Delta kL/2=\theta\Delta T$ where Δk is the phase-mismatch and L the crystal length.

The highest output power and efficiency were achieved with an output coupler of 10% transmittance at the laser wavelength and high reflectivity at the second harmonic. Figure 3 shows the measured average output power versus the incident pump power. The laser threshold is 3.7 W, while mode-locking is observed in the pump power range between 15.4 and 16.6 W. The maximum output power in the mode-locked regime was ~1 W, obtained at a pump level of 15.4 W. Higher output powers (up to 1.5 W) were generated increasing the incident pump power up to ~19 W. However, although the laser efficiency starts to decrease again, a second region of stable mode-locking operation was not observed, presumably because of the multimode character of the laser output at this pump level.

Downloaded from SPIE Digital Library on 25 Feb 2011 to 62.44.99.208. Terms of Use: http://spiedl.org/terms

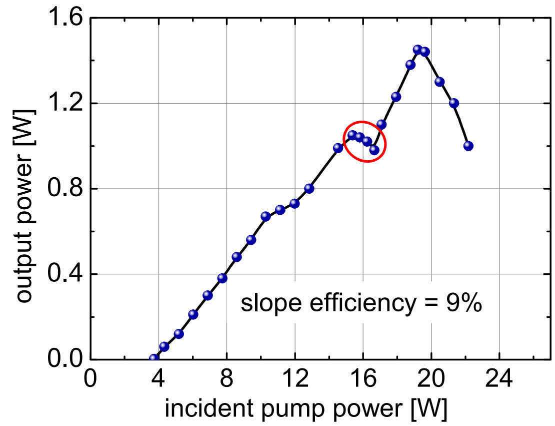

Fig. 3. Input-output characteristics of the $Nd:YVO_4$ laser with a 10% OC and PPMgSLT NLC. The mode-locking range is marked by the red oval.

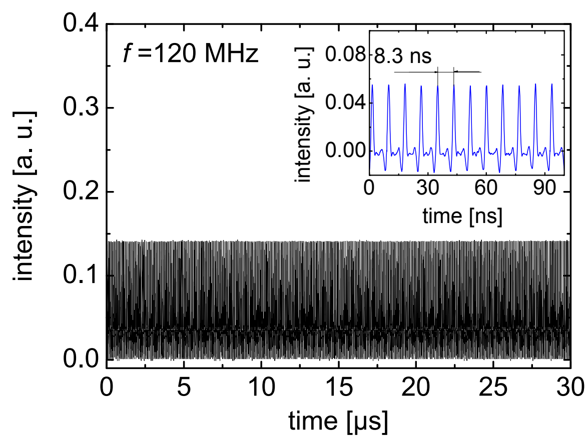

Fig. 4. Oscilloscope trace of the mode-locked pulse train obtained with the PPMgSLT NLC, recorded by a fast photodiode. The inset shows the individual pulses.

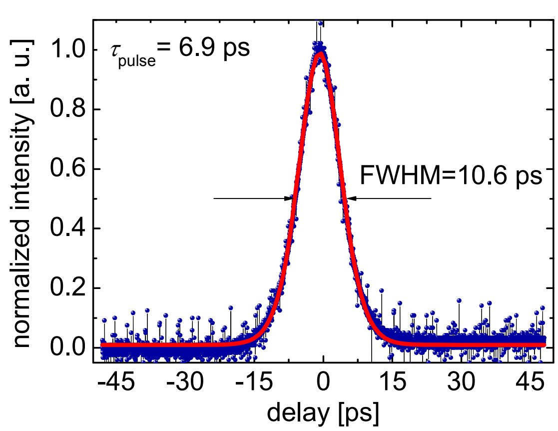

Fig. 5. Autocorrelation function (blue curve and symbols) and fit assuming $sech^2$ pulse shape (red curve) for the $Nd:YVO_4$ laser with a 10% OC and PPMgSLT NLC. The autocorrelation is measured by rotating-mirrors autocorrelator using non-collinear SHG in $LiIO_3$.

Downloaded from SPIE Digital Library on 25 Feb 2011 to 62.44.99.208. Terms of Use: http://spiedl.org/terms

A fast photodiode oscilloscope trace of the laser, mode-locked with PPMgSLT crystal, over a 30 μs time scale is shown in Fig. 4 together with the individual pulses.

Figure 5 shows the measured autocorrelation trace corresponding to maximum output power in the mode-locked regime. The fit, assuming sech^2 pulse shape, leads to an estimation of 6.9 ps for the pulse duration (FWHM). Somewhat shorter pulses (5.2 ps) where achieved by replacing the 10% output coupler with one having 5% transmittance at the fundamental and high reflection at the second harmonic. The shorter pulse duration obtained in this case is a consequence of the higher intra-cavity intensity, i.e. stronger $\chi^{(2)}$-nonlinear lens effect. However, the reduced transmission of the output coupler also leads to approximately 30% decrease in average output power in mode-locked operation.

In the case of BIBO, detuning from perfect phase-matching was achieved by changing the critical angle. Similarly, the phase-mismatched SHG introduces negative $\chi^{(2)}$-nonlinear lens in the laser resonator. Consequently, mode-locked operation was obtained only when tilting the nonlinear crystal in one direction, again far from perfect phase-matching.

The highest output power and efficiency with the BIBO NLC were achieved also with the 10% OC. The average power reached 1.3 W at an incident pump power of 12.5 W. The slope efficiency was 13.8%. The measured pulse duration in this case was slightly shorter, 5.3 ps, in comparison the PPMgSLT.

The shortest pulses with the BIBO NLC were obtained also using the 5% OC in which case the intacavity intensity was higher. Figure 6 shows the measured average output power versus the incident pump power in the case of the 5% OC. In this case the laser threshold was at 2.7 W and the mode-locking range in terms of incident pump power extended from 12 to 13.2 W. The maximum output power in mode-locked operation was again ~30% lower in comparison with the 10% OC, about 0.9 W, obtained at a pump level of 12.5 W. Higher average powers (~1.2 W) were obtained with this OC at increased pump power (up to ~17 W) but again, no second region of stable mode-locking operation was observed in this case.

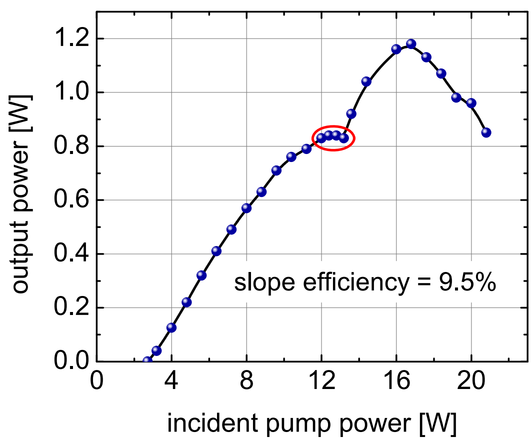

Fig. 6. Input-output characteristics of the Nd:YVO_4 laser with a 5% OC and BIBO NLC. The mode-locking range is marked by the red oval.

A fast photodiode oscilloscope trace of the laser, mode-locked with BIBO, over a 4 ms time scale (longer than the time scale for Q-switching and relaxation oscillations) is shown in Fig. 7 together with the individual pulses. No Q-switching instabilities are seen.

The measured FWHM of the autocorrelation trace, 5.7 ps, see Fig. 8, corresponds to a pulse duration (FWHM) of 3.7 ps assuming sech^2 pulse shape. These are the shortest pulses achieved so far for this transition of Nd-lasers by any mode-locking technique. Thus, in this first experiment BIBO produced shorter pulses than PPMgSLT. However, preliminary measurements using longer PPMgSLT samples, indicate that this nonlinear material can provide comparable pulse durations under similar experimental conditions.

Finally, Fig. 9 shows a photograph of the Nd:YVO_4 laser operating in the mode-locked regime.

Downloaded from SPIE Digital Library on 25 Feb 2011 to 62.44.99.208. Terms of Use: http://spiedl.org/terms

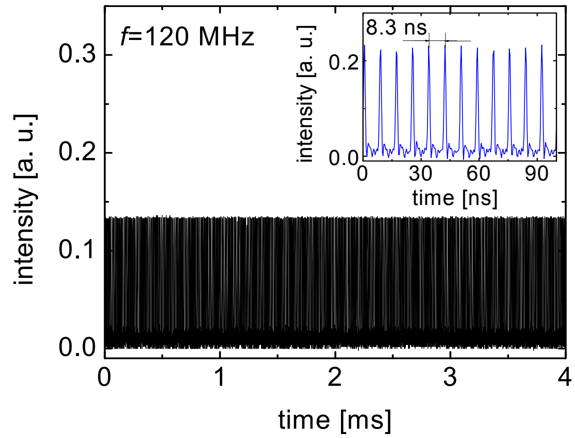

Fig. 7. Oscilloscope trace of the mode-locked pulse train obtained with the BIBO NLC, recorded by a fast photodiode. The inset shows the individual pulses.

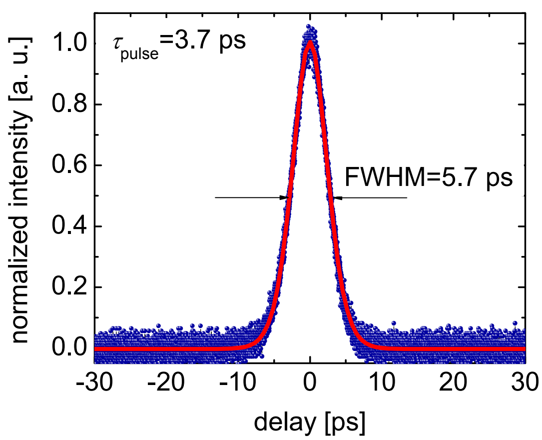

Fig. 8 Autocorrelation function (blue curve and symbols) and fit assuming $sech^2$ pulse shape (red curve) for the $Nd:YVO_4$ laser with a 5% OC and BIBO NLC. The autocorrelation is measured by rotating-mirrors autocorrelator using non-collinear SHG in $LiIO_3$.

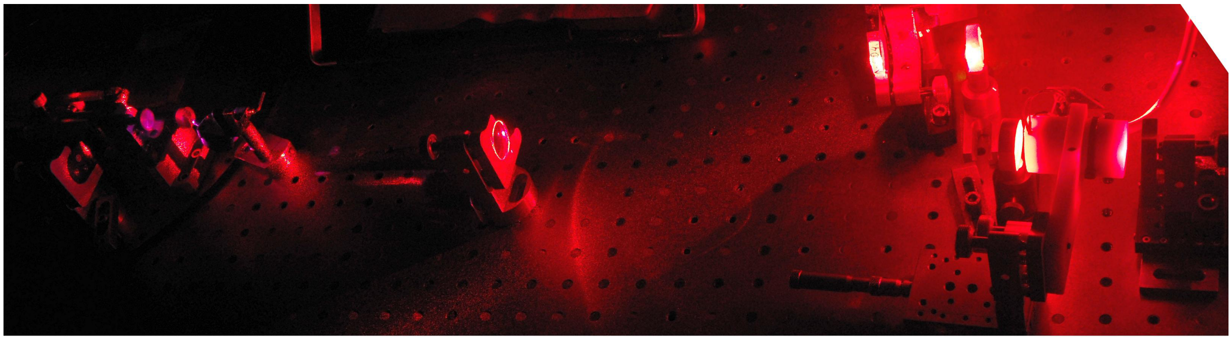

Fig. 9 Photograph of the operating $Nd:YVO_4$ laser in the mode-locked regime with PPMgSLT inside the cavity.

Downloaded from SPIE Digital Library on 25 Feb 2011 to 62.44.99.208. Terms of Use: http://spiedl.org/terms

4. CONCLUSION

In conclusion, we have demonstrated the first realization of a stable and self-starting 1.3 µm mode-locked Nd-laser using $\chi^{(2)}$-negative lens formation in PPMgSLT or BIBO intracavity nonlinear crystals. Such mode-locking is possible at pump power levels corresponding to the negative slope region of the input-output characteristics of the laser CW mode of operation. The average output power of the order of 1 W is limited by the achievable output power in stable TEM_{00} mode of operation in CW regime and further scaling should be possible by redesigning the laser cavity taking into account the thermal lens formation.

ACKNOWLEDGMENTS

This work has been supported by the Bulgarian Ministry of Science and Education under grants number VU-L-319/2007 and DO 02/134/2009, and by DAAD (Germany) under PPP program with grant number 50448357.

REFERENCES

1. G. P. A. Malcolm and A. I. Ferguson, "Mode-locking of diode laser-pumped solid-state lasers," Opt. Quantum Electron. **24**, 705-717 (1992).
2. D. A. Armstrong, A. Robertson, N. Langford, and A. I. Ferguson, "1.3-µm diode-pumped Nd:YLF additive-pulse mode-locked laser," in *Conference on Lasers and Electro-Optics*, Vol. 15 of 1995 OSA Technical Digest Series (Optical Society of America,Washington, D.C., 1995), pp. 344-345.
3. D. Krennrich, R. Knappe, B. Henrich, R. Wallenstein, and J. A. L'Huillier, „A comprehensive study of Nd:YAG, $Nd:YAlO_3$, $Nd:YVO_4$ and $Nd:GdVO_4$ lasers operating at wavelengths of 0.9 and 1.3 µm. Part 2: passively mode locked-operation," Appl. Phys. B **92**, 175-183 (2008).
4. R. Fluck, G. Zhang, U. Keller, K. J. Weingarten, and M. Moser, „Diode-pumped passively mode-locked 1.3-µm $Nd:YVO_4$ and Nd:YLF lasers by use of semiconductor saturable absorbers," Opt. Lett. **21**, 1378-1380 (1996).
5. H. D. Sun, G. J. Valentine, R. Macaluso, S. Calves, D. Burns, M. D. Dawson, T. Jouhti, and M. Pessa, "Low-loss 1.3-µm GaInNAs saturable Bragg reflector for high-power picosecond neodymium lasers," Opt. Lett. **27**, 2124-2126 (2002).
6. V. Liverini, S. Schön, R. Grange, M. Haiml, S. C. Zeller, and U. Keller, "Low-loss GaInNAs saturable absorber mode locking a 1.3-mm solid-state laser," Appl. Phys. Lett. **84**, 4002-4004 (2004).
7. K. W. Su, H. C. Lai, A. Li, Y. F. Chen, and K. F. Huang, "InAs/GaAs quantum-dot saturable absorber for a diode-pumped passively mode-locked $Nd:YVO_4$ laser at 1342 nm," Opt. Lett. **30**, 1482-1484 (2005).
8. S. L. Huang, H. L. Cheng, Y.-F. Chen, K. W. Su, Y. F. Chen, and K. F. Huang, „Diode-pumped passively mode-locked 1342 nm $Nd:YVO_4$ laser with an AlGaInAs quantum-well saturable absorber," Opt. Lett. **34**, 2348-2350 (2009).
9. S. J. Holmgren, V. Pasiskevicius, and F. Laurell, "Generation of 2.8 ps pulses by mode-locking a $Nd:GdVO_4$ laser with defocusing cascaded Kerr lensing in periodically poled KTP," Opt. Express **13**, 5270-5278 (2005).
10. H. Iliev, D. Chuchumishev, I. Buchvarov, and V. Petrov, "Passive mode-locking of a diode-pumped $Nd:YVO_4$ laser by intracavity SHG in PPKTP", Opt. Express **18**, 5754-5762 (2010).
11. H. Iliev, I. Buchvarov, S. Kurimura, and V. Petrov, "High-power picosecond $Nd:GdVO_4$ laser mode-locked by SHG in periodically-poled stoichiometric lithium tantalate", Opt. Lett. **35**, 1016-1018 (2010).
12. K. A. Stankov, V. Kubecek, and K. Hamal, "Mode-locking of a $Nd:YAlO_3$ laser at the 1.34-µm transition by a second-harmonic nonlinear mirror," Opt. Lett. **16**, 505-507 (1991).

13. A. Bruner, D. Eger, M. B. Oron, P. Blau, M. Katz, and S. Ruschin, ĂTemperature-dependent Sellmeier equation for the refractive index of stoichiometric lithium tantalate,ñ Opt. Lett. 28, 194-196 (2003).

Downloaded from SPIE Digital Library on 25 Feb 2011 to 62.44.99.208. Terms of Use: http://spiedl.org/terms